RSC Advances

This is an *Accepted Manuscript*, which has been through the Royal Society of Chemistry peer review process and has been accepted for publication.

Accepted Manuscripts are published online shortly after acceptance, before technical editing, formatting and proof reading. Using this free service, authors can make their results available to the community, in citable form, before we publish the edited article. This *Accepted Manuscript* will be replaced by the edited, formatted and paginated article as soon as this is available.

You can find more information about *Accepted Manuscripts* in the **Information for Authors**.

ROYAL SOCIETY
OF CHEMISTRY

www.rsc.org/advances

Optimal characteristic nanosizes of mineral bridges in mollusk nacre

Yue Shao,[1,2] Hong-Ping Zhao,[1] and Xi-Qiao Feng[1,3,]*

[1] Institute of Biomechanics and Medical Engineering, AML, Department of Engineering Mechanics, Tsinghua University, Beijing 100084, People's Republic of China

[2] Department of Mechanical Engineering, University of Michigan, Ann Arbor, MI 48109, USA

[3] Centre of Nano and Micro Mechanics, Tsinghua University, Beijing 100084, People's Republic of China

* Author to whom correspondence should be addressed. Electronic mail: fengxq@tsinghua.edu.cn.

ABSTRACT

To date, it is still unclear why all mineral bridges linking neighboring platelets in various types of mollusk nacres have sizes of 10–50 nanometers. We answer this question by investigating the strength of platelet-platelet interfaces, and found only when mineral bridges have diameters of a few tens nanometers, the interfaces can achieve an optimal strength. It is the uniformity of stress distributions in mineral bridges that dictates the selection of their characteristic sizes. The philosophy underlying interfacial optimization via mineral nanobridges simultaneously optimizes the load-bearing efficiency of materials. This study provides inspirations for biomimetic design of advanced composite materials.

After millions of years of evolution, natural biological materials have acquired superior mechanical properties via their elegant hierarchical structures from the nanoscale up.[1-4] Mounting evidence has suggested that nanosized structural features play a critical role in enhancing the strength of biological materials.[5-9] Investigations on the size effect of microstructures in biological materials could help to reveal novel strengthening strategies adopted by nature, and provide inspirations for biomimetic design of high-performance engineering materials.[10-13]

Nacre (or the mother-of-pearl) has attracted the interest and security of many scientists because of its outstanding mechanical strength and fracture toughness in comparison to those of its constituent counterparts, which mainly include aragonite (~ 95% vol.) and protein-rich organic phase (~ 5% vol.) assembled in a hierarchical fashion.[14-22] At the micro scale, nacre has an elegant "brick-and-mortar" structure, which is composed of microsized mineral platelets ("bricks") interspersed in an organic matrix ("mortar").[14,15,17] At the nano scale, the mineral platelets are composed of aragonite nanograins, which are the structural elements in the growth of nacre.[16,17,21,22] As a critical connection, the structural transition from mineral nanograins to microsized platelets and the "brick-and-mortar" structure in nacre is mediated by the formation of nanosized mineral bridges at the platelet-platelet interfaces.[16,17] Interestingly, the diameters of mineral bridges in various types of mollusk nacre all fall in a narrow range of 10–50 nm.[23-27] Regarding the superior mechanical properties of nacre, previous studies have revealed a number of strengthening mechanisms across multiple length scales,[4,19,23,24,27-37] among which an optimal strength of platelet-platelet interfaces is of critical importance.[37,38] However, it is still unclear whether and how the characteristic nanosizes (10–50 nm) of mineral bridges in nacre help to

optimize the platelet-platelet interface strength, which further contributes to the outstanding macroscopic mechanical properties of nacre.

To answer this question, we here establish a theoretical model to investigate the size effect of mineral bridges on the interface strength in nacre. According to our dimensional analysis and finite element simulations, it is the optimization of platelet-platelet interface strength under shear that dictates the characteristic sizes of mineral bridges in the range of about 10–40 nm, in consistency with relevant experimental observations. By analyzing the stress distribution and the material's load-bearing efficiency, the mechanisms underlying the size effect of mineral bridges are also revealed, providing insights for innovative design of high-strength engineering materials mimicking the interface nanostructures in nacre.

On the basis of experimental observations, a theoretical model is established for the microstructure of nacre (Figure 1). It is composed of a periodic array of mineral bridges linking two neighboring platelets in nacre (Figure 1a,c). According to the tension-shear chain model of nacre, the platelet-platelet interfaces predominantly transfer shear stresses.[29] Therefore, we focus on the interface strength under remote shear stress, τ, applied to the mineral platelets sandwiching the interfacial layer. On the basis of previous experimental observations, individual mineral bridge has curvilinear morphology[23,25-27] and is approximated in our model by a columnar structure with meniscus-like exterior surfaces of curvature radius $h/2$, where h is the thickness of the two-phase interface layer (Figure 1b,d). To investigate the size effect of mineral bridges, their characteristic size is defined by the diameter of their minimal cross-section, $2a$. In this model, the interstitial space outside the mineral phase is occupied by the soft organic phase, separating neighboring mineral bridges by periodicity $2c$. It is notable that the dimensionless parameter a/c characterizes the volume percentage of mineral phase in the interfacial layer.

3

Therefore, we define *a/c* as a constant in the following analysis in order to provide a control, demonstrating that the size effect we study is not due to simply changing the amount of load-bearing mineral phase in the interface. To keep it as that observed in nacre, we choose the ratio *a/c* to be 1/3, reflecting the bridge-bridge distance about 50 – 80 nm and average bridge diameter as 25 nm.[24,27] Furthermore, since the organic phase is softer than the mineral phase by a factor of $10^2 - 10^3$,[19,39] its effect on the interfacial stress is negligible (as we will demonstrate below) and the externally applied shear load is mainly undertaken by the mineral bridges. In the following analysis, we only incorporate the mechanical property of the mineral phase unless mentioned otherwise. For the sake of simplicity, we will first focus on the two-dimensional (2D) model (Figure 1), and the main conclusions drawn from 2D analysis will be demonstrated also in the three-dimensional (3D) case.

Recent experiments showed that the aragonite phase in nacre is not just a simple brittle monocrystal but composed of nanocrystal grains.[21,22] In addition, the pure aragonite may undergo a certain amount of nanoscale ductile deformation.[40] Therefore, we reckon it is necessary to include the possibility of ductile failure of nanosized mineral bridges into our model. In particular, we study the interface strength under external shear loading before the occurrence of yielding of mineral bridges, and choose the maximal von Mises equivalent stress, σ_{max}^{Mises}, as the failure criterion. It is a function of the following parameters:

$$\sigma_{max}^{Mises} = f\left(a, c, h, H, \tau, E\right), \tag{1}$$

where *a* is the radius of the mineral bridge at the minimal cross section, *c* is the spacing between two neighboring mineral bridges, *h* is the interface thickness or the mineral bridge height, τ is the remote shear stress, 2*H* is the thickness of a mineral platelet due to the top-bottom symmetry of our model (Figure 1a), and *E* is the Young's modulus of the mineral material. The mineral phase,

including the mineral bridges and platelets, is treated as a homogeneous and linear elastic material with Poisson's ratio $\nu = 0.3$. Using the Pi theorem for dimensional analysis, Eq. (1) reduces to a dimensionless function:

$$\frac{\sigma_{max}^{Mises}}{\tau} = f^*\left(\frac{a}{c}, \frac{a}{h}, \frac{a}{H}, \frac{\tau}{E}\right). \tag{2}$$

Since a/c is taken as a constant and $a/H << 1$, Eq. (2) can be simplified as

$$\frac{\sigma_{max}^{Mises}}{\tau} = f^*\left(\frac{a}{h}, \frac{\tau}{E}\right). \tag{3}$$

Thus the failure of the mineral phase depends only on two normalized parameters, a/h and τ/E. The former describes the geometric feature of the mineral bridges, and the latter stands for their mechanical property. Given the linear elasticity of the mineral phase and the complete force boundary condition in the interface model, the theory of elasticity concludes that the stress solution for the problem is independent of the elastic modulus, E.[41] Thus, one has

$$\frac{\sigma_{max}^{Mises}}{\tau} = f^*\left(\frac{a}{h}\right), \tag{4}$$

suggesting a size effect wherein the internal stress and failure of mineral bridges depend mainly on a single normalized geometric parameter, a/h.

To verify the above conclusion derived from dimensional analysis, 2D plane-strain numerical simulations are performed to calculate the stress distribution by using the software Abaqus 6.9.1. For the microstructure-based model for the platelet–platelet interface illustrated in Figure. 1, the stress state within the mineral bridge is determined from the finite element simulations. Considering the periodic boundary conditions, we only calculate a representative volume element of the interface, as shown in Figure 1b. Although geometric nonlinearity has been implemented in the finite element simulations, the numerical results (Figure 2a) agree well

with our result from dimensional analysis based on the theory of linear elasticity. This shows that the maximal von Mises stress $\sigma_{\mathrm{max}}^{\mathrm{Mises}}$ is indeed independent of the elastic modulus E of the mineral phase but highly sensitive to the change in the characteristic size of mineral bridges, a/h. The value of $\sigma_{\mathrm{max}}^{\mathrm{Mises}}$ decreases with decreasing a/h and reaches an asymptotic value when a/h is smaller than 0.6 (Figure 2a).

In this study, we assume that a mineral bridge will start to fail when its maximal von Mises stress $\sigma_{\mathrm{max}}^{\mathrm{Mises}}$ reaches the critical value σ_{b}. Thus the interface strength, τ_{b}, is defined as the remote shear stress satisfying this critical condition. Since the yield stress of a material is usually smaller than the elastic modulus by orders of magnitude,[42] we take the yield stress as $\sigma_{\mathrm{b}}/E = 1/200$, which is estimated from previous experimental reports[43] and represented by a hyperbola in Figure 2a. Therefore, the interface strength τ_{b} can be determined as the critical shear stress in Figure 2a where each horizontal line meets the yielding curve. It is emphasized that so far we have kept the theoretical model as dimensionless in order to demonstrate the dominant role of mineral bridge aspect ratio a/h in interface strength, as well as the generality of our model potentially for guiding interface design at different length scales. In the following, however, we will introduce nacre-specific parameters and length scale to understand how the mineral bridges of diameters 10 – 50 nm specifically affect the interface strength in nacre.

To more clearly reveal the size effect by the nanosized mineral bridges, we calculate the failure strength of the interface via finite element simulations. On the basis of relevant experiments of nacre, we take the following representative values: E = 80 GPa,[43] $\sigma_{\mathrm{b}}^{\mathrm{Mises}}$ = 400 MPa (tensile strength estimated as a fraction of measured compressive strength of 1 GPa),[43] h = 25 nm, H = 300 nm,[18,19] and $c = 3a$.[27] The characteristic size $2a$ is varied in the range from 14 to

200 nm, wherein the lower limit of $2a$ is determined by the geometric feature of the mineral bridge and the periodicity in our interface model. Figure 2b gives the simulation results regarding the dependence of interface strength, τ_b, on the mineral bridge diameter $2a$. It is clear that τ_b increases almost linearly as the size of mineral bridges shrinks, and it reached a plateau only when the diameter of mineral bridge is around or smaller than 40 nm. This result unequivocally shows that the characteristic nanometer sizes of mineral bridges usually observed in nacre, i.e., 10–50 nm in diameter, belongs to an optimal range of sizes that maximizes the interface strength under shear. As is well known, enhancing the interface at nanoscale is of crucial significance for improving the macroscopic tensile strength of materials. In addition, our simulations show that the incorporation of a soft organic phase[39] with $E_{organic}/E = 0.001$ and $\nu_{organic} = 0.49$ has negligible influence on the interface strength (Figure 2b), justifying our approach that only considers the mechanical property of the mineral phase. It is also notable that unlike many size effects of nanomaterials resulting from surface effect, the size effects and the optimal interface strength revealed in this study raise mainly from the nanosized geometry of mineral bridges and the strength optimization of the nanostructured interface in nacre.

Further, to gain insights into the mechanisms underlying the size effect described above, we look into the stress state within individual mineral bridges, the most important load-bearing elements in platelet-platelet interfaces. In particular, we examine the von Mises stress distribution across the critical plane within a mineral bridge, where the maximal stress and failure starts to occur (Figure 3a, inset). The simulation results in Figure 3a clearly demonstrate that the uniformity of stress distribution within the mineral bridge is dependent of its sizes. The global stress distribution becomes more and more uniform as the mineral bridge diameter $2a$ decreases down to a value of 50 nm, echoing the linear increase in interface strength in Figure 2b.

However, when $2a$ is smaller than 50 nm, the stress distribution in the vicinity of the ends continues becoming more uniform while that in the central region undergoes de-unification as the size decreases further. Therefore, the two counteracting trends might cancel out and result in the plateau for the size effect when the diameter of mineral bridges reaches the optimal range between 10 and 40 nm (Figure 2b).

In principle, more uniform distribution of stress suggests more efficient usage of the material. Here we introduce the following parameter to describe the load-bearing efficiency of material:

$$\varepsilon_{avg} = \frac{S_{eff}}{S_{total}} = \frac{1}{S_{total}} \int_{critical\ plane} \frac{\sigma^{Mises}(S)}{\sigma_{b}^{Mises}} dS \qquad (5)$$

where $\sigma^{Mises}(S)$ is the distribution of von Mises stress in the critical plane, S_{eff} the effective load-bearing area, and S_{total} the total area in the critical plane. The parameter ε_{avg} reflects the average usage of the load-bearing potential of mineral phase in the critical plane of individual mineral bridges. It is calculated from the stress distribution curve in the critical plane. Figure 3b illustrates the relation between the normalized material efficiency $\bar{\varepsilon}_{avg}$ and the mineral bridge diameter $2a$. An optimal efficiency is found when the diameter is smaller than 40 nm, reflecting a similar size effect as observed in Figure 2b. In fact, the relation between the normalized effective load-bearing area $\bar{S}_{eff}$ and the mineral bridge diameter $2a$ is also plotted in Figure 3b. It also illustrates a similar size effect as $\bar{\varepsilon}_{avg}$ although they have a slight difference. This difference is due to the fact that the critical plane is offset from the mid-plane of the mineral bridge (Figure 3a, inset) because of its curvilinear morphology and thus the total area of critical plane, S_{total}, undergoes a slight variation for different mineral bridge sizes. Both size effects in $\bar{\varepsilon}_{avg}$ and $\bar{S}_{eff}$

reflect the intrinsic optimization mechanism of interface strength and thus implicates that the optimal characteristic size of mineral bridges is determined by the size-dependent uniformity of stress distribution and the load-bearing efficiency of material in the nanostructured interface. In other words, if the mineral bridge diameter is larger than 50 nm, higher stress concentration would appear, lowering both the load-bearing ability of platelet–platelet interfaces and the overall utilization efficiency of material. By contrast, the mineral bridges in the size range of 10 – 50 nm readers to uniform stress distribution and optimal interface properties.

Additionally, to verify that the size effect and the optimal interface strength mechanism derived from the 2D model have a general meaning, we build three-dimensional (3D) finite element models (Figure 4a). Using the same values of parameters given above, the results from 3D simulations are shown in Figure 4b. It is clear that our conclusions obtained in 2D context are confirmed by 3D simulations. In spite of that the numerical values of 2D and 3D results have slight difference, they do share the same optimal characteristic size range of mineral bridges, 10– 40 nm, which correlates with the optimal strength of interfaces (Figure 4b). This result verifies that the difference between 2D and 3D models have no significant effect on the conclusions, which thus holds the potential of the size effect and our biomimetic philosophy in helping designing and optimizing real 3D-structured interfaces.

In summary, we have unraveled a size effect of nanoscale mineral bridges in nacre. It is found that the mineral bridges diameter in the range of about 10–40 nm can optimize the interface strength. This size effect is attributed to the nanostructure of platelet–platelet interfaces. The size-dependent uniformity of stress distribution and the load-bearing efficiency of material are identified as dominant mechanisms underlying the size effect by mineral bridges. The results could deepen our understanding of the role of nanostructures in regulating interface mechanics in

natural biological materials and also provide clues for design and fabrication of materials mimicking their nanostructured interfaces.

REFERENCES

(1) Fratzl, P.; Weinkamer, R. Nature's Hierarchical Materials. *Prog. Mater. Sci.* **2007**, *52*, 1263-1334.

(2) Meyers, M. A.; Chen, P. Y.; Lin, A. Y. M.; Seki, Y. Biological Materials: Structure and Mechanical Properties. *Prog. Mater. Sci.* **2008**, *53*, 1-206.

(3) Espinosa, H. D.; Rim, J. E.; Barthelat, F.; Buehler, M. J. Merger of Structure and Material in Nacre and Bone - Perspectives on *De Novo* Biomimetic Materials. *Prog. Mater. Sci.* **2009**, *54*, 1059-1100.

(4) Mayer, G. New Toughening Concepts for Ceramic Composites from Rigid Natural Materials. *J. Mech. Behav. Biomed. Mater.* **2011**, *4*, 670-681.

(5) Arzt, E. Biological and Artificial Attachment Devices: Lessons for Materials Scientists from Flies and Geckos. *Mat. Sci. Eng. C* **2006**, *26*, 1245-1250.

(6) Gao, H. J.; Yao, H. M. Shape Insensitive Optimal Adhesion of Nanoscale Fibrillar Structures. *Proc. Natl. Acad. Sci. U. S. A.* **2004**, *101*, 7851-7856.

(7) Keten, S.; Xu, Z. P.; Ihle, B.; Buehler, M. J. Nanoconfinement Controls Stiffness, Strength and Mechanical Toughness of Beta-Sheet Crystals in Silk. *Nature Mater.* **2010**, *9*, 359-367.

(8) Buehler, M. J. Tu(R)Ning Weakness to Strength. *Nano Today* **2010**, *5*, 379-383.

(9) Launey, M. E.; Buehler, M. J.; Ritchie, R. O. On the Mechanistic Origins of Toughness in Bone. *Ann. Rev. Mater. Res.* **2010**, *40*, 25-53.

(10) Barthelat, F. Biomimetics for Next Generation Materials. *Philos. Trans. R. Soc. A* **2007**, *365*, 2907-2919.

(11) Bhushan, B. Biomimetics: Lessons from Nature - an Overview. *Philos. Trans. R. Soc. A* **2009**, *367*, 1445-1486.

(12) Podsiadlo, P.; Kaushik, A. K.; Arruda, E. M.; Waas, A. M.; Shim, B. S.; Xu, J. D.; Nandivada, H.; Pumplin, B. G.; Lahann, J.; Ramamoorthy, A.; Kotov, N. A. Ultrastrong and Stiff Layered Polymer Nanocomposites. *Science* **2007**, *318*, 80-83.

(13) Bonderer, L. J.; Studart, A. R.; Gauckler, L. J. Bioinspired Design and Assembly of Platelet Reinforced Polymer Films. *Science* **2008**, *319*, 1069-1073.

(14) Currey, J. D. Mechanical-Properties of Mother of Pearl in Tension. *Proc. R. Soc. B* **1977**, *196*, 443-463.

(15) Jackson, A. P.; Vincent, J. F. V.; Turner, R. M. The Mechanical Design of Nacre. *Proc. R.*

Soc. B **1988**, *234*, 415-440.

(16) Addadi, L.; Joester, D.; Nudelman, F.; Weiner, S. Mollusk Shell Formation: A Source of New Concepts for Understanding Biomineralization Processes. *Chem. Eur. J.* **2006**, *12*, 981-987.

(17) Lin, A.; Meyers, M. A. Growth and Structure in Abalone Shell. *Mat. Sci. Eng. A* **2005**, *390*, 27-41.

(18) Barthelat, F.; Espinosa, H. D. An Experimental Investigation of Deformation and Fracture of Nacre-Mother of Pearl. *Exp. Mech.* **2007**, *47*, 311-324.

(19) Barthelat, F.; Tang, H.; Zavattieri, P. D.; Li, C. M.; Espinosa, H. D. On the Mechanics of Mother-of-Pearl: A Key Feature in the Material Hierarchical Structure. *J. Mech. Phys. Solids* **2007**, *55*, 306-337.

(20) Barthelat, F. Nacre from Mollusk Shells: A Model for High-Performance Structural Materials. *Bioinspir. Biomim.* **2010**, *5*, 035001.

(21) Li, X. D.; Chang, W. C.; Chao, Y. J.; Wang, R. Z.; Chang, M. Nanoscale Structural and Mechanical Characterization of a Natural Nanocomposite Material: The Shell of Red Abalone. *Nano Lett.* **2004**, *4*, 613-617.

(22) Huang, Z. W.; Li, X. D. Origin of Flaw-Tolerance in Nacre. *Sci. Rep.* **2013**, *3*, 1693.

(23) Song, F.; Bai, Y. L. Effects of Nanostructures on the Fracture Strength of the Interfaces in Nacre. *J. Mater. Res.* **2003**, *18*, 1741-1744.

(24) Song, F.; Zhou, J. B.; Xu, X. H.; Xu, Y.; Bai, Y. L. Effect of a Negative Poisson Ratio in the Tension of Ceramics. *Phys. Rev. Lett.* **2008**, *100*, 245502.

(25) Gries, K.; Kröger, R.; Kübel, C.; Schowalter, M.; Fritz, M.; Rosenauer, A. Correlation of the Orientation of Stacked Aragonite Platelets in Nacre and Their Connection Via Mineral Bridges. *Ultramicroscopy* **2009**, *109*, 230-236.

(26) Checa, A. G.; Cartwright, J. H. E.; Willinger, M. G. Mineral Bridges in Nacre. *J. Struct. Biol.* **2011**, *176*, 330-339.

(27) Song, F.; Soh, A. K.; Bai, Y. L. Structural and Mechanical Properties of the Organic Matrix Layers of Nacre. *Biomaterials.* **2003**, *24*, 3623-3631.

(28) Okumura, K.; de Gennes, P. G. Why Is Nacre Strong? Elastic Theory and Fracture Mechanics for Biocomposites with Stratified Structures. *Eur. Phys. J. E* **2001**, *4*, 121-127.

(29) Gao, H. J. Application of Fracture Mechanics Concepts to Hierarchical Biomechanics of

Bone and Bone-Like Materials. *Int. J. Fract.* **2006**, *138*, 101-137.

(30) Rabiei, R.; Bekah, S.; Barthelat, F. Failure Mode Transition in Nacre and Bone-Like Materials. *Acta Biomater.* **2010**, *6*, 4081-4089.

(31) Barthelat, F.; Rabiei, R. Toughness Amplification in Natural Composites. *J. Mech. Phys. Solids* **2011**, *59*, 829-840.

(32) Wang, R. Z.; Gupta, H. S. Deformation and Fracture Mechanisms of Bone and Nacre. *Ann. Rev. Mater. Res.* **2011**, *41*, 41-73.

(33) Barthelat, F.; Dastjerdi, A. K.; Rabiei, R. An Improved Failure Criterion for Biological and Engineered Staggered Composites. *J. R. Soc. Interface* **2013**, *10*, 20120849.

(34) Rim, J. E.; Zavattieri, P.; Juster, A.; Espinosa, H. D. Dimensional Analysis and Parametric Studies for Designing Artificial Nacre. *J. Mech. Behav. Biomed. Mater.* **2011**, *4*, 190-211.

(35) Espinosa, H. D.; Juster, A. L.; Latourte, F. J.; Loh, O. Y.; Gregoire, D.; Zavattieri, P. D. Tablet-Level Origin of Toughening in Abalone Shells and Translation to Synthetic Composite Materials. *Nat. Commun.* **2011**, *2*, 173.

(36) Katti, K. S.; Katti, D. R.; Pradhan, S. M.; Bhosle, A. Platelet Interlocks Are the Key to Toughness and Strength in Nacre. *J. Mater. Res.* **2005**, *20*, 1097-1100.

(37) Shao, Y.; Zhao, H. P.; Feng, X. Q.; Gao, H. J. Discontinuous Crack-Bridging Model for Fracture Toughness Analysis of Nacre. *J. Mech. Phys. Solids* **2012**, *60*, 1400-1419.

(38) Shao, Y.; Zhao, H. P.; Feng, X. Q. On Flaw Tolerance of Nacre: A Theoretical Study. *J. R. Soc. Interface* **2014**, *11*, 20131016.

(39) Ji, B. H.; Gao, H. J. Mechanical Properties of Nanostructure of Biological Materials. *J. Mech. Phys. Solids* **2004**, *52*, 1963-1990.

(40) Kearney, C.; Zhao, Z.; Bruet, B. J. F.; Radovitzky, R.; Boyce, M. C.; Ortiz, C. Nanoscale Anisotropic Plastic Deformation in Single Crystal Aragonite. *Phys. Rev. Lett.* **2006**, *96*, 255505.

(41) Landau, L. D.; Lifshitz, E. M. *Theory of Elasticity*; Pergamon Press: Oxford, 1970.

(42) Currey, J. D.; Brear, K. Hardness, Young's Modulus and Yield Stress in Mammalian Mineralized Tissues. *J. Mater. Sci. - Mater. Med.* **1990**, *1*, 14-20.

(43) Barthelat, F.; Li, C. M.; Comi, C.; Espinosa, H. D. Mechanical Properties of Nacre Constituents and Their Impact on Mechanical Performance. *J. Mater. Res.* **2006**, *21*, 1977-1986.

Figure Captions

Figure 1. 2D model for a platelet–platelet interface with mineral bridges in nacre. (a) Interface with a periodic array of mineral bridges (*blue*) interspersed in a soft organic phase (*yellow*). (b) Zoom-in schematic of a representative volume element (*dashed blue box in (a)*) of the interface. (c) Scanning transmission electron microscopy (STEM) image of platelet–platelet interface in nacre. Array of mineral bridges was observed in the interfacial layer. Adapted with permission.[25] (d) TEM image of a single mineral bridge between mineral platelets (boundary of the mineral phase marked by *yellow dashed lines*). Adapted with permission.[26]

Figure 2. Theoretical and numerical results of size effect. (a) Finite element results on the relation between the reduced maximal von Mises stress $\sigma_{\max}^{\text{Mises}}/\tau$ and the normalized shear stress τ/E. Effect of the reduced mineral bridge size a/h is illustrated as separated curves, and the yield condition (*orange curve*) is also plotted. (b) Finite element results for the relation between the interface strength τ_b and the nanosizes of mineral bridges. The results both with and without the soft organic phase are shown. The yellow line is drawn for the guidance of eyes. The inset shows 2D finite element models.

Figure 3. Size-dependent stress distribution and load-bearing efficiency of material. (a) Normalized distribution of von Mises stress σ^{Mises} across the critical plane (*inset, orange lines*) in the mineral bridge of different sizes. (b) Variation of normalized materials efficiency $\bar{\varepsilon}_{\text{avg}}$ and normalized effective load-bearing area $\bar{S}_{\text{eff}}$ with respect to the mineral bridge size.

Figure 4. 3D finite element simulation results. (a) Left: 3D interface model with a periodic array of mineral bridges (*blue*) between two neighboring platelets, and right: zoom-in schematic of a representative element of the interface model. The organic phase filling the interstitial space is not shown for the sake of clarity. (b) Simulation results showing the dependence of interface strength on the mineral bridge size. The yellow line is drawn for the guidance of eyes.
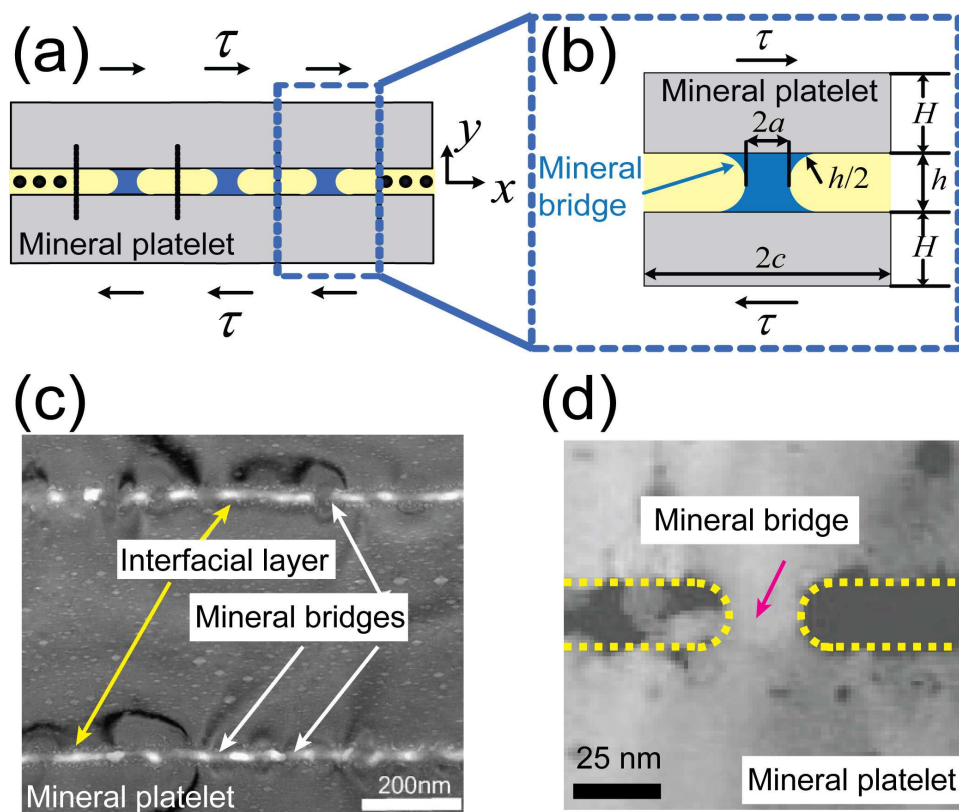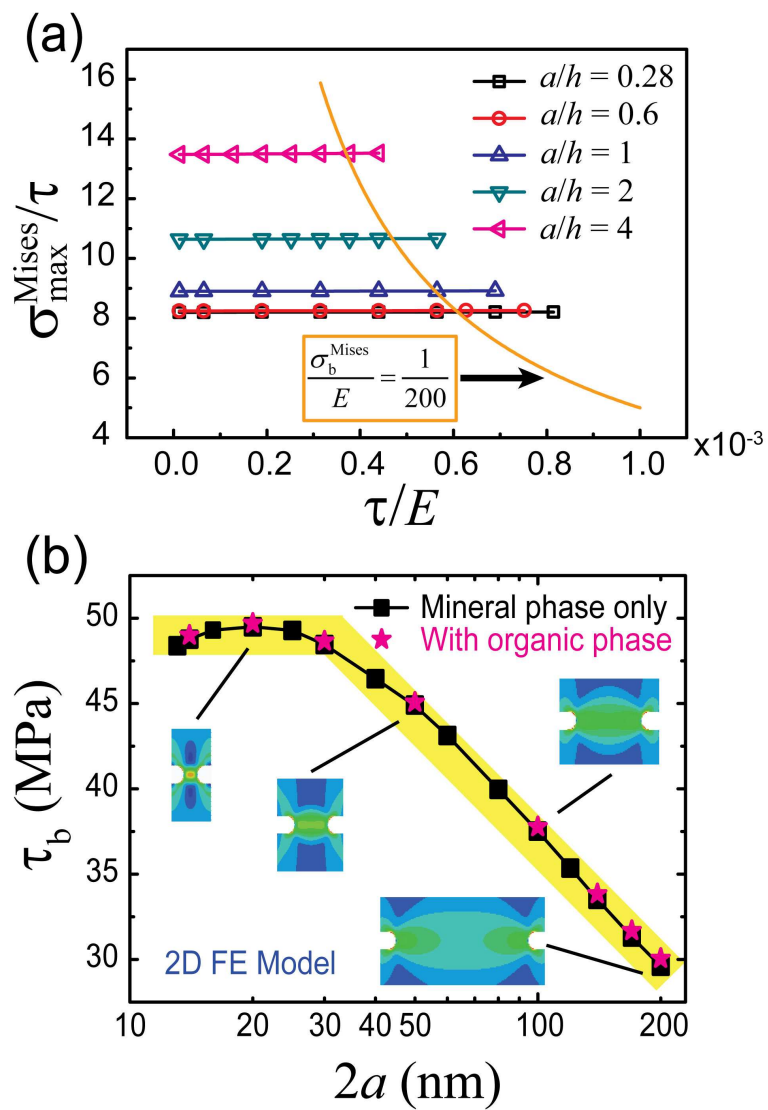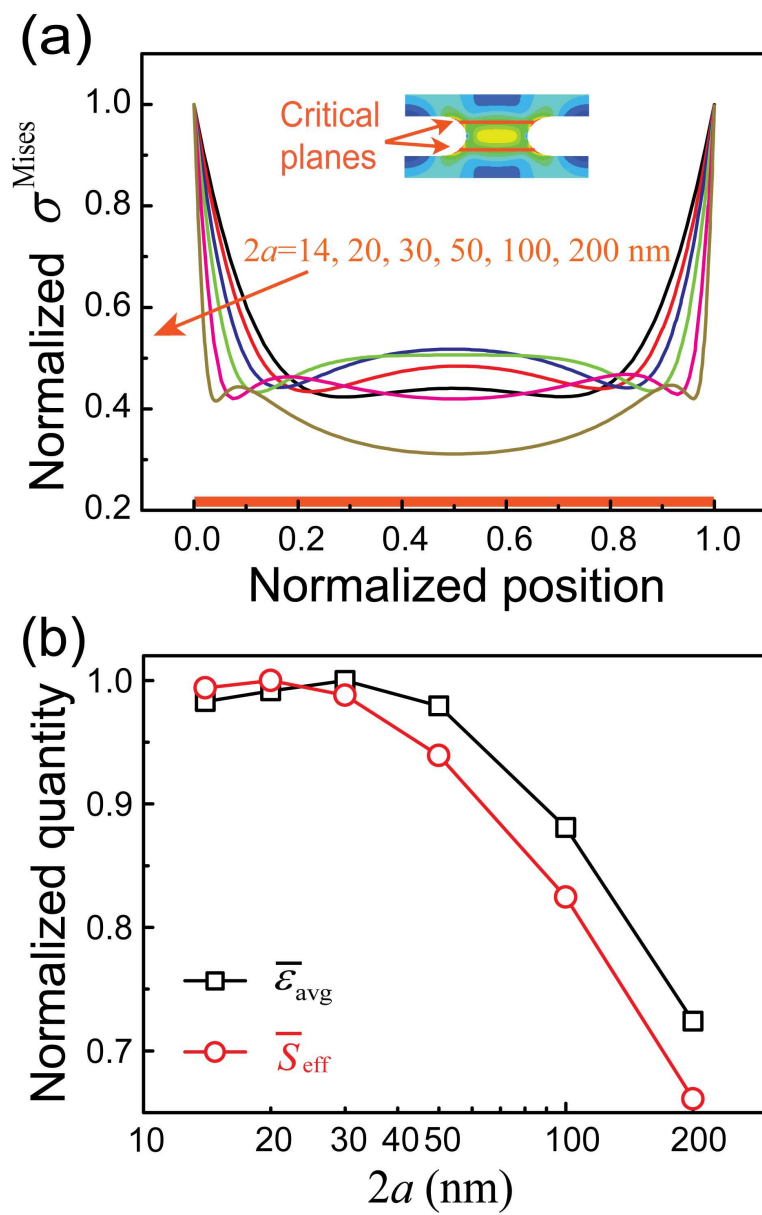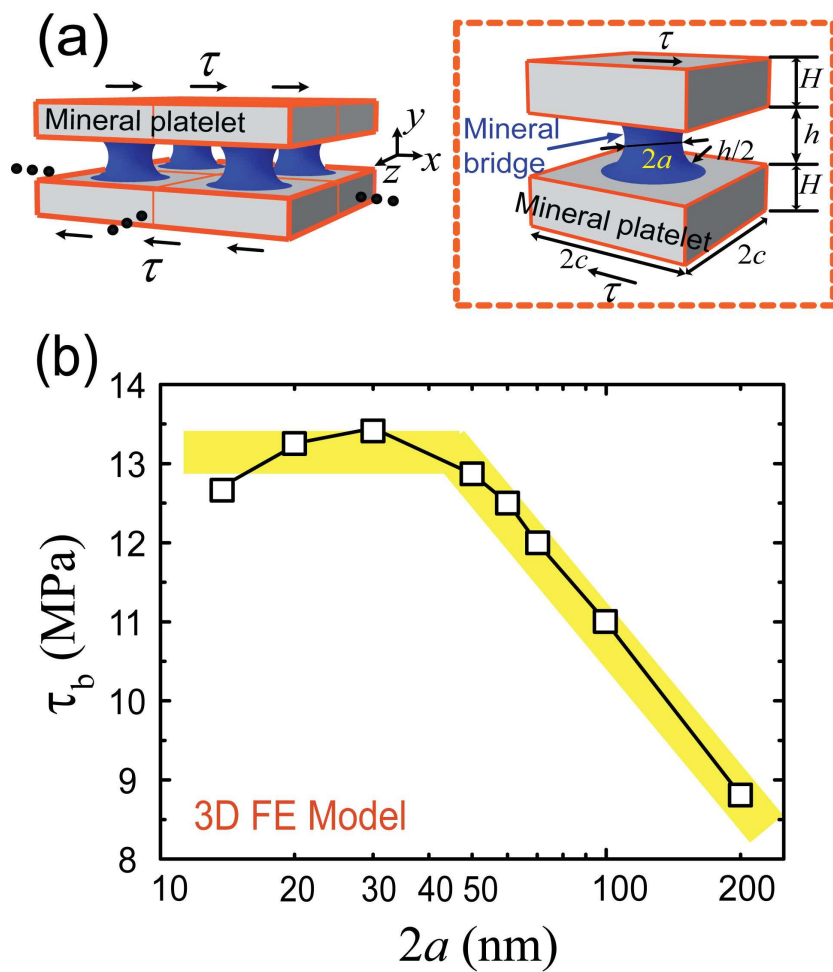
Figures

Figure 1

Figure 2

Figure 3

3

(a)

Mineral platelet

Mineral bridge

Mineral platelet

(b)

3D FE Model

Figure 4

4

Graphical Abstract

Nacre-mimick interface

Shear

Mineral platelet

Shear

Interface strength

Nanobridge sizes (aspect ratio)
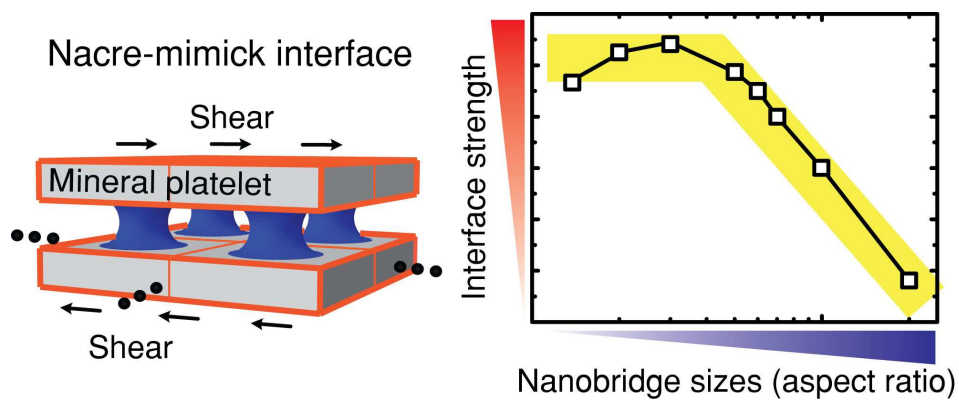
The nanosizes of mineral bridges linking neighboring platelets in various types of mollusk nacres dictates the optimal interfacial strength.